CHARACTERIZATION OF A NEW ORGANIC-CATION CYCLOTETRAPHOSPHATE : $[NH_3(CH_2)_4NH_3]_2P_4O_{12}.9/2H_2O$

H. THABET*, M. BDIRI*, A. JOUINI* (1), A. DURIF**

*Laboratoire de chimie du solide, Département de chimie, Faculté des sciences de Monastir, 5000 Monastir, Tunisie.
**Laboratoire de cristallographie, CNRS associé à l'université J.-Fourier, BP 166, 38042 Grenoble Cedex 09, France.

(Soumis en décembre 1994, accepté en octobre 1995)

ABSTRACT. Chemical preparation, differential scanning calorimetric analysis, IR spectrometric investigation and crystal structure are given for a new organic condensed phosphate. The putrescinium cyclotetraphosphate hydrate $[NH_3(CH_2)_4NH_3]_2P_4O_{12}.9/2H_2O$ is monoclinic C2/c with Z=8 and unit cell dimensions: a=38.87(2)Å, b=9.478(2)Å, c=13.97(2)Å, β=96.51(7)°. The structure was refined to a final Rw value of 0.031. The atomic arrangement is a typical layer organization built by alternating layers of anions and cations. The anion layers, including P_4O_{12} rings and water molecules, are in planes centred on z=1/4 and 3/4, while the cation layers, made up by the three independent putrescinium dications $[NH_3(CH_2)_4NH_3]^{2+}$, are in planes centred on z=0.0 and 1/2. All the N-H···O hydrogen bonds are established between adjacent layers while the O-H···O bonds operate within the anionic layer linking (i) two P_4O_{12} groups to form clusters: $[(P_4O_{12})_2(H_2O)_3]^{8-}$, (ii) clusters to form infinite ribbons: $[(P_4O_{12})_2(H_2O)_7]_n^{8n-}$ and (iii) ribbons to form an infinite two-dimensional layer. The DSC study shows that the dehydration occurs in three steps. Such dehydration process may be related to the different environments of the water molecules in H-bond schemes. The reported IR investigation, indicates a satisfactory agreement between the predicted, on the basis of a group theoretical analysis, and the observed P_4O_{12} stretching bands, especially in the 800-600 cm^{-1} characteristic region for C_1 symmetry.

RÉSUMÉ. La préparation chimique, et les caractérisations physico-chimique et structurale sont données pour un nouveau phosphate condensé organique: $[NH_3(CH_2)_4NH_3]_2P_4O_{12}.9/2H_2O$ de groupe d'espace C2/c avec Z=8 et les paramètres de maille a=38,87(2)Å, b=9,478(2)Å, c=13,97(2)Å, β=96,51(7)°. L'arrangement atomique présente une organisation typique en couches alternatives d'anions et de cations. Les couches anioniques formées par de P_4O_{12} et de molécules d'eau, sont centrées par les plans en z=1/4 et 3/4, alors que les couches cationiques, formées de $[NH_3(CH_2)_4NH_3]^{2+}$, sont dans les plans en z=0.0 et 1/2. La cohésion entre couches successives est maintenue par les liaisons hydrogène du type N-H···O . Les laisons hydrogène du type O-H···O

(1) To whom correspondence should be addressed.

agissent de trois façons, au sein de la couche anionique, en liant: (i) deux groupements P_4O_{12} pour former des clusters $[(P_4O_{12})_2(H_2O)_3]^{8-}$, (ii) les clusters pour former des rubans infinis $[(P_4O_{12})_2(H_2O)_7]_n^{8n-}$ et (iii) les rubans pour former une couche bidimensionnelle infinie. L'analyse calorimétrique différentielle montre que la déshydtratation se produit en trois étapes. Le processus de cette déshydratation peut être reliée aux différents environnements des molécules d'eau. L'investigation par spectrométrie IR indique un accord satisfaisant entre les vibrations de valence prévues par la théorie des groupes et observées dans P_4O_{12}, en particulier, dans la région 800-600 cm^{-1} caractéristique de la symétrie C_1.

I- INTRODUCTION

The investigations of hydrated organic condensed phosphates have shown the great ability of P_4O_{12} groups to build, through hydrogen bonds, frameworks with organic cations [1],[2], in particular, for materials resulting from the interaction between cyclotetraphosphoric acid and alkyl diamines, with general formula, $NH_2(CH_2)_nNH_2$. The three previously characterized structures in this field are those of $[NH_2\text{-}NH_3]_4P_4O_{12}$ [3], $[NH_3(CH_2)_2NH_3]_2\ P_4O_{12}.2H_2O$ [4] and $[NH_3(CH_2)_3NH_3]_2P_4O_{12}.2H_2O$ [5] corresponding to n=0, 2 and 3. Putrescine, $NH_2(CH_2)_4NH_2$ with the extension to n=4, is a linear biogenic diamine. It is present as a diprotonated cation in biological systems and interacts with nucleic acids through H-bonding. Putrescine interaction with phosphoric acids led, up to now, to three well characterized atomic arrangements: $[NH_3(CH_2)_4NH_3](H_2PO_4)_2$ [6],[7], $[NH_3(CH_2)_4NH_3]HPO_4.2H_2O$ [8] and $[NH_3(CH_2)_4NH_3]H_2P_2O_7$ [9]. These structure studies showed that the putrescinium dication, in the solid state, has a strong preference to be located around crystallographic centres [6],[7], [9-12]. If it was located in a general position, this dication would be found in a symmetric conformation with a non-crystallographic centre [13]. This ability to be highly symmetric is related to the geometrical flexibility, as the putrescinium dication has been found in the extended all-trans conformation. This work is devoted to the structural investigation of the putrescinium cyclotetraphosphate. The chemical preparation, crystallo-graphic features, detailed DSC and IR spectrometric analysis are reported.

II-EXPERIMENTAL

A. Chemical preparation

Chemical preparation has been performed in two steps; first a concentrated solution of $H_4P_4O_{12}$ is prepared by passing an aqueous solution of $Na_4P_4O_{12}$ through an ion-exchange resin, Amberlite IR 120, in its H-form. The resulting solution is then neutralized by a stoichiometric quantity of 1,4-butanediamine (Fluka Chemika, > 97%). These two steps are performed at room temperature. Schematically the reaction is :

$$H_4P_4O_{12} + 2NH_2(CH_2)_4NH_2 \xrightarrow{H_2O} [NH_3(CH_2)_4NH_3]_2\ P_4O_{12}.9/2H_2O$$

The solution is then slowly evaporated at room temperature. After several days of evaporation, the crystallization of $[NH_3(CH_2)_4NH_3]_2\ P_4O_{12}.9/2H_2O$ occurs as colorless elongated monoclinic prisms

B. Chemical analysis and thermal behaviour

The chemical analysis of phosphorus has been carried out by using a UV-spectrometer 190 SHIMADZU, that of protons by a volumetric method [14]. The thermogravimetric analysis was done with the help of a thermoanalyzer SETARAM G70. Experiments were performed with a specimen of 100 mg in an open silica crucible and heated from 298 to 700 K in air. Differential calorimetric analysis was carried out using a SETARAM DSC 92 and weighed 10-15 mg purified samples sealed in an aluminium DSC crucible; an empty aluminium crucible was used as a reference. Samples were heated from 298 to 500 K in air using various heating rates.

C. Structure determination

The parameters used for the X-ray diffraction data collection, as well as the strategy used for the crystal structure determination and its final results are reported in table I. Twenty reflections ($10.2 < \theta < 11.8$) were used for refining the unit-cell dimensions. Density was measured at room temperature using toluene as pycnometric liquid The final atomic coordinates for non-H atoms and their equivalent temperature factors are given in table II. The values of the thermal anisotropic displacement parameters for non-H atoms, final coordinates and isotropic thermal factors for H-atoms, list of observed and calculated structure factors are available on request.

D. Infrared spectroscopic investigation

IR spectra were recorded by using a SHIMADZU CHART 200-91527 spectrometer. Samples were dispersed in KBr and scanning performed in the 4000 - 400 cm^{-1} spectral domain with a resolution of about 3 cm^{-1}.

III-STRUCTURE DESCRIPTION

This atomic arrangement is a typical layer organization built by two types of layers. The first type of layer made by the $P_4O_{12}^{4-}$ ring anions and the water molecules is approximately centred on planes z = 1/4 and 3/4 ; the second type of layer, parallel to the first one, but centred on planes z=0 and 1/2, includes the three crystallographic independent organic groups. Figure 1 reporting this arrangement in projection along the **b** axis shows clearly the layered organization of its various components.

The first type of layer can be described by a stacking of clusters, $[(P_4O_{12})_2(H_2O)_3]^{8-}$ built by two P_4O_{12} groups and three water molecules interconnected by H-bonds. These clusters, with a twofold internal symmetry, are themselves linked by the strongest H-bonds observed in this arrangement so as to build ribbons parallel to the b axis. Inside a ribbon,

Table I: *Main crystallographic features, parameters used for the X-ray diffraction data collection, strategy used for the crystal structure determination and its final results.*

I. Crystal data	
Formula:$(C_4H_{14}N_2)_2P_4O_{12}.9/2H_2O$	Fw = 577.3
Crystal system : monoclinic	Space group : C2/c
a = 38.87(2), b = 9.478(2)	V = 5116(12)Å^3
c = 13.97(2) Å, β = 96.51(7)°	Z = 8
Unit cell refined from 20 reflections	(10.2 < θ < 11.8°)
$\rho_{cal.}$ = 1.499 , $\rho_{obs.}$ = 1.49 g.cm^{-3}	F(000) = 2440
Linear absorption factor :	μ(AgKα) = 0.201 mm^{-1}
Morphology :	elongated monoclinic prism
Crystal size :	0.45x 0.45x 0.32 mm
II. Intensity measurements	
Temperature : 298K	Wavelength: AgK_α(0.5608Å)
Diffractometer : Nonius CAD4	Scan mode : ω
Monochromator : graphite plate	Scan width : 1.20°
Variable scan speed	$T_{max.}$ per scan : 60 s
Theta range :	2-27.5°
Background measuring time :	T_{max} /2
Measurement area : ±h, k, l	$h_{max.}$=62, $k_{max.}$=15, $l_{max.}$=19
Number of scanned reflections :	12441
Number of non-zero reflections :	6831
Number of unique reflections :	6559 (Rint= 0.01)
Reference reflections :	every 2hr, no variation
III. Structure determination	
Lorentz and polarization corrections:	No absorption correction
Program used : SDP [15]	Computer used: Micro-Vax II
Unique reflections included :	6559 (no rejection)
Weighting scheme : unitary	Refined parameters : 442
Secondary extinction coefficient:	not applied
Unweighted agreement factor R :	0.029
Weighted agreement factor Rw :	0.031
Esd : 1.722	Largest shift/error = 0.04
Max. residual density :	0.38 e.Å^{-3}

Table II: *Final atomic coordinates and for non-H atoms. Estimated standard deviations are given in parentheses.*

Atom	x(σ)	y(σ)	z(σ)	Beq.(σ)
P(1)	0.41203(1)	0.26815(4)	0.29931(3)	1.674(5)
P(2)	0.09422(1)	0.47624(4)	0.27557(2)	1.460(5)
P(3)	0.17120(1)	0.49713(4)	0.30522(3)	1.553(5)
P(4)	0.33607(1)	0.27036(4)	0.29093(3)	1.537(5)
O(E11)	0.43582(3)	0.3773(1)	0.2696(1)	2.88(2)
O(E12)	0.41645(3)	0.2090(1)	0.39774(8)	2.39(2)
O(L12)	0.41172(3)	0.1425(1)	0.22072(7)	2.00(2)
O(L41)	0.37341(3)	0.3305(1)	0.27421(8)	1.95(2)
O(E21)	0.07287(3)	0.4108(1)	0.19212(7)	1.96(2)
O(E22)	0.09120(3)	0.4225(1)	0.37406(7)	2.04(2)
O(L23)	0.13344(2)	0.4622(1)	0.25079(7)	1.81(2)
O(E31)	0.19632(3)	0.4354(1)	0.24435(8)	2.32(2)
O(E32)	0.17331(3)	0.4585(1)	0.40827(7)	2.27(2)
O(L34)	0.32819(3)	0.1665(1)	0.20005(8)	2.13(2)
O(E41)	0.31167(3)	0.3903(1)	0.27633(9)	2.52(3)
O(E42)	0.33769(3)	0.1877(1)	0.38166(7)	1.97(2)
O(W1)	0.25438(4)	0.3214(2)	0.3704(1)	4.50(3)
O(W2)	0.99251(4)	0.5276(2)	0.3778(2)	4.10(3)
O(W3)	0.05097(5)	0.1544(2)	0.2748(1)	4.92(4)
O(W4)	0.500	0.2565(2)	0.250	5.36(6)
O(W5)	0.17823(6)	0.1435(2)	0.2994(2)	8.37(5)
N(1)	0.11854(3)	0.4484(1)	0.04464(9)	2.04(2)
N(2)	0.13467(4)	0.1888(1)	0.4402(1)	2.53(3)
N(3)	0.03070(4)	0.2892(2)	0.4431(1)	2.53(2)
N(4)	0.27532(3)	0.0405(1)	0.4265(1)	2.33(2)
C(1)	0.13851(4)	0.3157(2)	0.0409(1)	2.44(3)
C(2)	0.11594(5)	0.1932(2)	0.0059(1)	2.68(3)
C(3)	0.13772(5)	0.0617(2)	-0.0071(1)	2.70(3)
C(4)	0.11489(5)	0.0577(2)	0.4521(1)	2.80(3)
C(5)	0.00185(4)	0.1948(2)	0.4634(1)	2.93(3)
C(6)	0.48515(4)	0.4519(2)	0.5106(1)	2.89(3)
C(7)	0.25204(4)	0.4385(2)	0.0521(1)	2.67(3)
C(8)	0.23636(4)	0.2999(2)	0.0158(1)	2.70(3)

$$B_{eq.} = 4/3 \sum_i \sum_j a_i . b_j . \beta_{ij}$$

each cluster is connected to its adjacent neighbor through four water molecules. These infinite ribbons $[(P_4O_{12})_2\ (H_2O)_7]_n^{8n-}$ are linked so as to form an infinite layer by additional water molecules. Inside such a layer, each ribbon is related from its neighbor through the 2_1 helical axis. Figure 2 reports in projection along the c axis the organization of the layer centred on the plane z = 1/4.

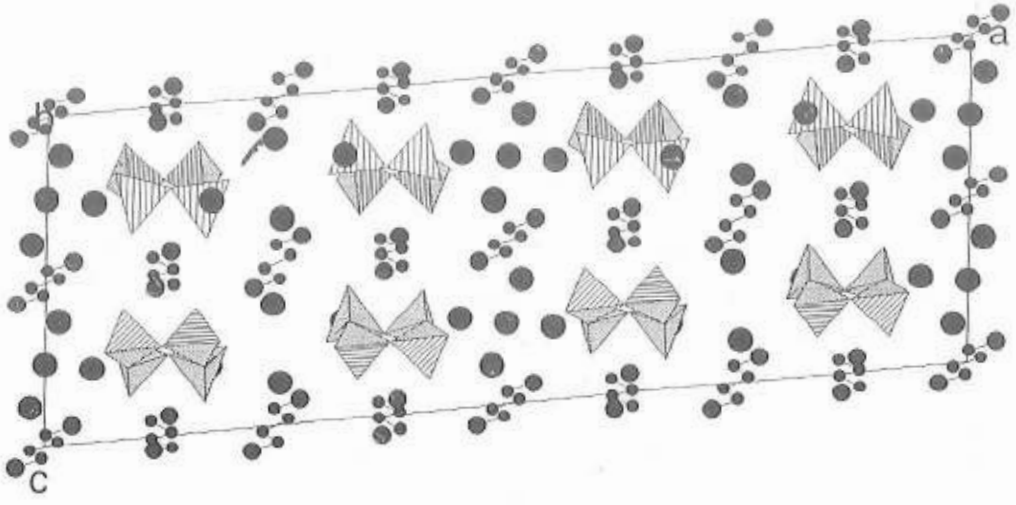

Figure 1: *Projection along the* **b** *direction of the atomic arrangement. Cyclotetraphosphate groups are given with a polyhedral representation. By order of decreasing sizes, black circles represent water molecules, nitrogen and carbon atoms. Hydrogen atoms have been omitted.*

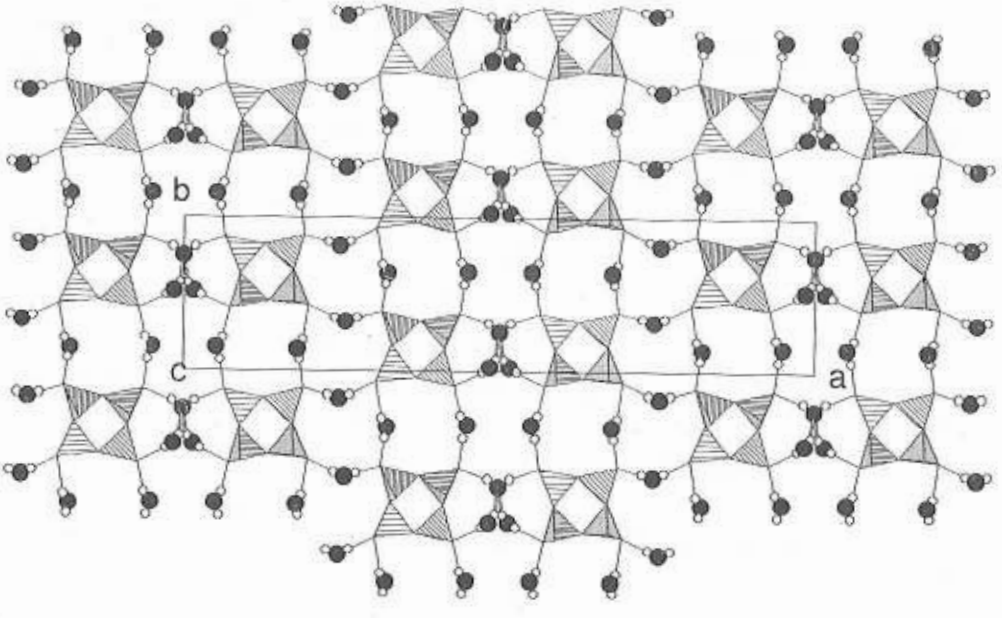

Figure 2: *Projection along the* **c** *direction of the anionic layer located around the plane z = 1/4. The P_4O_{12} groups are given in polyhedral representation. The black circles represent the water-oxygen atoms, the white smaller the hydrogen atoms. Hydrogen bonds are dotted.*

The second type of layer is a stacking made by the three crystallographic independent putrescinium dications. One of them, found in a general position and built up by C(1), C(2), C(3), C(4), N(1) and N(2), is strongly pseudocentrosymmetric with a pseudo inversion centre at 1/8,1/8,0. The two others comprising C(5), C(6), N(3) and C(7), C(8), N(4) are centrosymmetric and are located around the crystallographic inversion centres at 0,0,0 and 1/4,1/4,0 in the fully extended all-trans conformation. The torsion angles N(1)-C(1)-C(2)-C(3), N(3)-C(5)-C(6)-C'(6) and N(4)-C(7)-C(8)-C'(8) are respectively 174.1(1)°, 179.7(1)° and 174.3(1)°. Nevertheless, the main geometrical features of these three groups, reported in table III, do not differ significantly and are in accordance with all previously reported data [6-9]. Figure 3 reports, in projection along the **c** direction, the organic layer centred on the plane z = 0. In such a layer, the extended all-trans conformations are practically aligned along the **b** axis and organized to form infinite isolated organic entities spreading along the [1 1 0] direction.

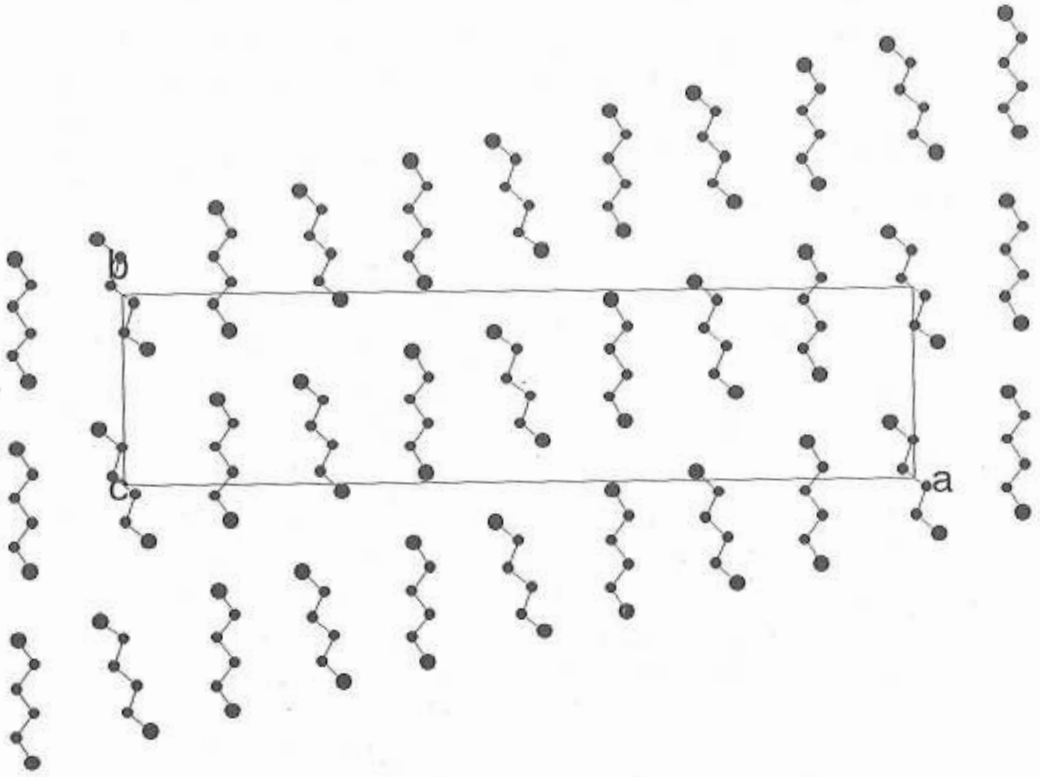

Figure 3: *Projection along the **c** direction of the putrescinium layer located around the plane z = 0.0. The larger black circles are nitrogen atoms and the smaller circles represent carbon atoms. Hydrogen atoms have been omitted.*

The $P_4O_{12}^{4-}$ ring anion involved in the inorganic layer has no local symmetry and in fact no specific features when compared with what is

commonly observed for this type of anionic entity, except the relatively important departure of the P-P-P angles (87.17-93.26°) from the ideal value (90°). In spite of this distortion the four P-atoms are approximately coplanar. Table III. reports the main geometrical features of the phosphoric ring anion.

Table III: *Main interatomic distances (Å) and bond angles (°). Estimated standard deviations are given in parentheses.*

The P_4O_{12} ring anion

The $P(1)O_4$ tetrahedron

P(1)	O(E11)	O(E12)	O(L12)	O(L41)
O(E11)	1.4779(9)	121.14(6)	106.29(5)	106.18(5)
O(E12)	2.574(1)	1.4777(9)	110.10(5)	110.39(5)
O(L12)	2.480(1)	2.540(1)	1.6191(8)	100.76(5)
O(L41)	2.474(1)	2.540(1)	2.491(1)	1.6146(8)

The $P(2)O_4$ tetrahedron

P(2)	O(E21)	O(E22)	O(L12)	O(L23)
O(E21)	1.4880(8)	119.22(5)	111.55(5)	104.77(4)
O(E22)	2.564(1)	1.4847(8)	106.36(5)	110.38(5)
O(L12)	2.550(1)	2.466(1)	1.5945(8)	103.50(4)
O(L23)	2.452(1)	2.539(1)	2.514(1)	1.6065(8)

The $P(3)O_4$ tetrahedron

P(3)	O(E31)	O(E32)	O(L23)	O(L34)
O(E31)	1.4859(9)	119.52(5)	105.77(5)	110.66(5)
O(E32)	2.562(1)	1.4792(8)	110.96(5)	106.99(5)
O(L23)	2.469(1)	2.544(1)	1.6094(8)	101.62(4)
O(L34)	2.545(1)	2.482(1)	2.493(1)	1.6076(9)

The $P(4)O_4$ tetrahedron

P(4)	O(E41)	O(E42)	O(L41)	O(L34)
O(E41)	1.4792(8)	119.16(5)	106.48(5)	107.42(5)
O(E42)	2.557(1)	1.4856(8)	111.16(5)	109.72(5)
O(L41)	2.469(1)	2.547(1)	1.6011(8)	101.37(5)
O(L34)	2.490(1)	2.531(1)	2.483(1)	1.6085(9)

P(1)-P(2)	2.9583(4)	P(2)-P(1)-P(4)	87.18(1)
P(1)-P(4)	2.9418(4)	P(1)-P(2)-P(3)	91.60(1)
P(2)-P(3)	2.9805(4)	P(2)-P(3)-P(4)	87.23(1)
P(3)-P(4)	2.9165(4)	P(1)-P(4)-P(3)	93.23(1)

P(1)-O(L12)-P(2)	134.01(5)	P(3)-O(L34)-P(4)	130.14(6)
P(2)-O(L23)-P(3)	135.88(5)	P(1)-O(L41)-P(4)	132.37(5)

Table III (continuation)

The putrescinium groups

N(1)-C(1)	1.482(2)	N(1)-C(1)-C(2)	112.2(1)
C(1)-C(2)	1.503(2)	C(1)-C(2)-C(3)	110.9(1)
C(2)-C(3)	1.529(2)	C(2)-C(3)-C(4)	110.2(1)
C(3)-C(4)	1.509(2)	N(2)-C(4)-C(3)	112.4(1)
C(4)-N(2)	1.481(2)		
N(3)-C(5)	1.487(2)	N(3)-C(5)-C(6)	111.2(1)
C(5)-C(6)	1.510(2)	C(5)-C(6)-C(6)	110.9(2)
C(6)-C(6)	1.525(3)		
N(4)-C(7)	1.493(2)	N(4)-C(7)-C(8)	111.2(1)
C(7)-C(8)	1.511(2)	C(7)-C(8)-C(8)	111.7(1)
C(8)-C(8)	1.523(3)		

The cohesion between the different layers is performed by N–H···O hydrogen-bonds connecting the hydrogen atoms of the NH_3 radicals to the external oxygen atoms of the phosphoric rings or to the water molecules. Geometrical details of the hydrogen-bond scheme are listed in table IV.

IV-THERMAL BEHAVIOUR

The TG thermogram, reproduced in figure 4, shows two separated weigh losses of water:

$$[C_4H_{14}N_2]_2P_4O_{12}.9/2H_2O \xrightarrow{373K} [C_4H_{14}N_2]_2P_4O_{12}.2H_2O \xrightarrow{453K} [C_4H_{14}N_2]_2P_4O_{12}$$

The first step corresponds to the loss of 2.5 water molecules in the range 353-410 K with a maximum at 373 K; the second, to the loss of the two remaining water molecules in the range 413-473 K with a maximum at 453 K. But in the DTG curve (fig.4) the first step appears as a practically symmetric peak while the second one, leading to the complete dehydration, is present as a shouldered peak. However we observe in the DSC thermogram (fig.5) three separated endothermic transformations in the temperature range 338-441 K corresponding to the complete dehydration of the compound. The two first endothermic peaks can be correlated to the first symmetric peak observed in DTG curve and probably attributed to the loss of water molecules linking ribbons in inorganic layers and clusters in a ribbon. The remaining shouldered endothermic peak, as detected in DTG curve, corresponds to a gradual removal of the 1.5 water

molecules that link two anionic groups into a cluster. This tentative explanation takes into account the strong effects of hydrogen bonds involving phosphate groups. Thus, the difference between measured values of ΔH corresponding respectively to the three endothermic peaks (21.2, 67.2 and 115.3 $KJ.mol^{-1}$) indicates the large degree of retention that water molecules exhibit.

Table IV: *Bond lengths (Å) and angles (°) in the hydrogen-bonding scheme; e.s.d.'s are given in parentheses.*

	N-H O-H	H···O	N-O O-O	N-H···O O-H···O
N(1)-H(1N1)···O(E42)	0.89(2)	2.07(2)	2.950(1)	173(2)
N(1)-H(2N1)···O(E22)	0.87(2)	1.93(2)	2.781(1)	167(2)
N(1)-H(3N1)···O(E21)	0.88(2)	2.05(2)	2.891(1)	160(1)
N(2)-H(1N2)···O(E42)	0.90(2)	1.97(2)	2.849(1)	166(2)
N(2)-H(2N2)···O(W5)	0.82(2)	1.96(2)	2.770(2)	167(2)
N(2)-H(3N2)···O(E22)	0.94(2)	1.95(2)	2.874(1)	168(2)
N(3)-H(1N3)···O(W3)	0.89(2)	2.00(2)	2.864(2)	165(1)
N(3)-H(2N3)···O(E12)	0.87(2)	1.99(2)	2.852(1)	170(2)
N(3)-H(3N3)···O(W2)	0.87(2)	1.96(3)	2.799(2)	159(2)
N(4)-H(1N4)···O(W1)	0.83(2)	2.04(2)	2.867(2)	173(2)
N(4)-H(2N4)···O(E31)	0.91(2)	2.01(2)	2.916(2)	172(2)
N(4)-H(3N4)···O(E32)	0.88(2)	2.01(2)	2.877(1)	168(2)
O(W1)-H(1OW1)···O(E41)	0.85(2)	1.95(2)	2.789(2)	171(2)
O(W1)-H(2OW1)···O(E31)	0.81(2)	2.10(2)	2.909(2)	172(2)
O(W2)-H(1OW2)···O(W4)	0.80(2)	2.08(2)	2.847(2)	161(2)
O(W2)-H(2OW2)···O(E21)	0.84(2)	2.01(2)	2.842(2)	174(2)
O(W3)-H(1OW3)···O(E11)	0.88(3)	1.89(3)	2.761(2)	169(2)
O(W3)-H(2OW3)···O(E21)	0.90(3)	2.02(3)	2.862(2)	155(2)
O(W4)-H(OW4)···O(E11)	0.87(2)	1.96(2)	2.786(1)	159(2)
O(W5)-H(1OW5)···O(E31)	0.73(3)	2.31(3)	2.978(2)	154(3)
O(W5)-H(2OW5)···O(E41)	0.76(3)	1.92(3)	2.670(2)	174(3)

H(1OW1)-O(W1)-H(2OW1) 113(2)	H(1OW2)-O(W2)-H(2OW2) 107(2)
H(1OW3)-O(W3)-H(2OW3) 106(2)	H(OW4)-O(W4)-H(OW4) 107(3)
H(1OW5)-O(W5)-H(2OW5) 111(3)	

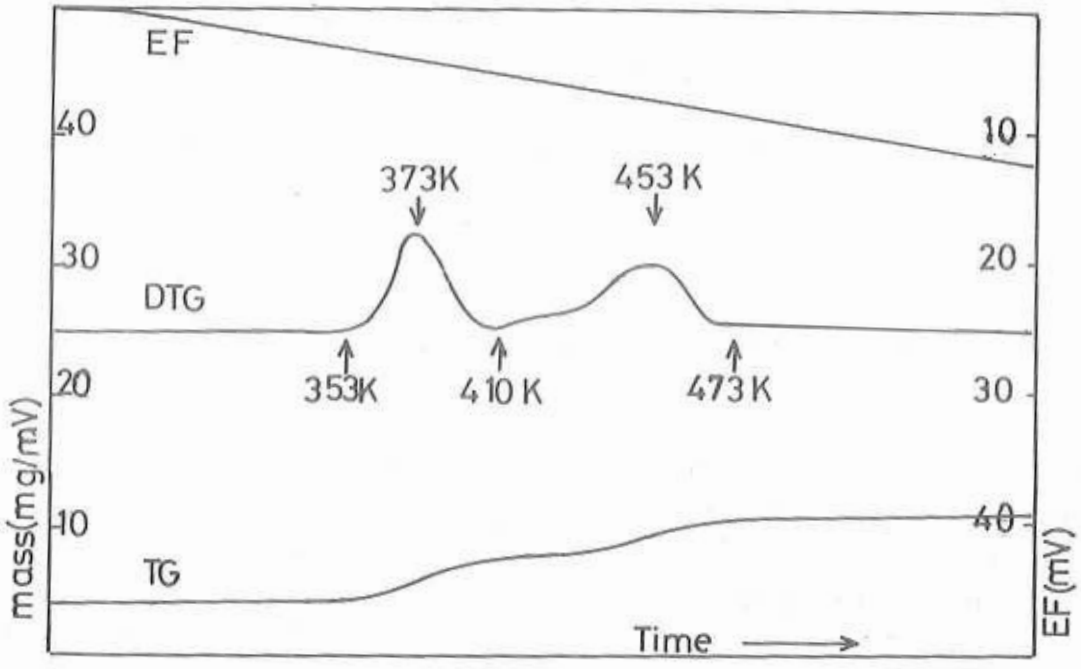

Figure 4: *TGA thermogram of $[NH_3(CH_2)_4NH_3]_2P_4O_{12}.9/2H_2O$*

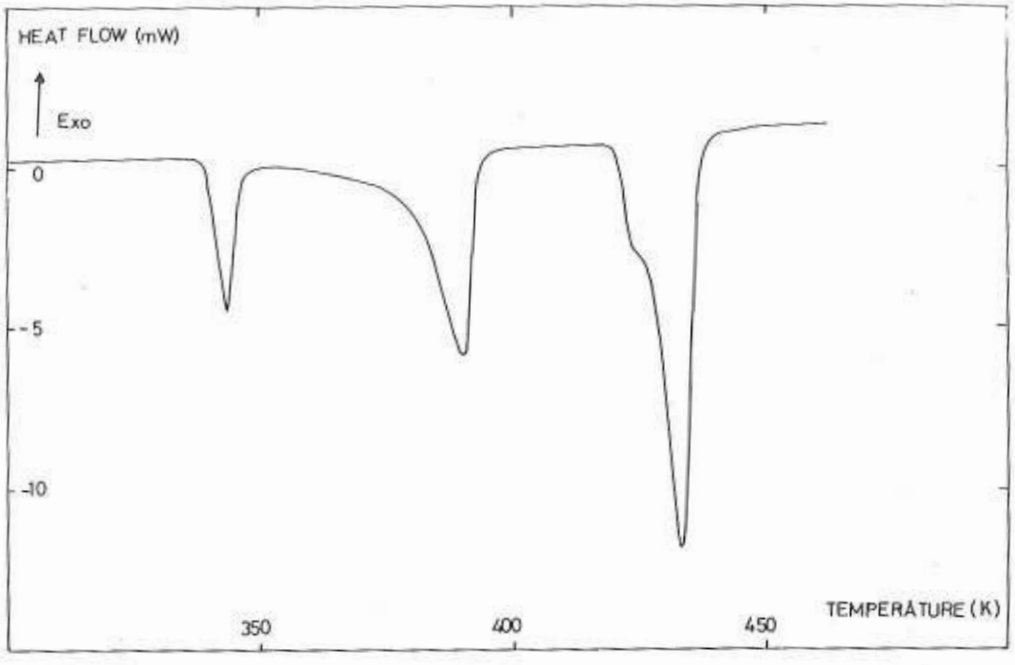

Figure 5: *Differential scanning calorimetry for a polycristalline sample of $[NH_3(CH_2)_4NH_3]_2P_4O_{12}.9/2H_2O$; heating rate 3°/min.*

V-INFRARED INVESTIGATION

In the crystal, the $P_4O_{12}^{4-}$ ring anions occupy a site C_1 of lower symmetry than the S_4 symmetry observed in $SrK_2P_4O_{12}$ [16], but the latter presents the advantage of having one formula unit only in the crystallographic cell. A typical IR-spectrum of the title compound is represented in figure 6. The observed frequencies, in the P_4O_{12} stretching region, are collected in table V. The proposed assignments are deduced from the following bases:

(i) Since the isolated P_4O_{12} ring belongs to the C_1 symmetry group, all the 16 fundamental stretching vibrations predicted by theoretical group analysis are non-degenerate modes, active in the IR as well as in the Raman.

(ii) According to previous studies [16-19], the stretching P-O modes of the P_4O_{12} ring will be found in the following sequence: $\nu_{as}OPO^- > \nu_sOPO^- > \nu_{as}POP > \nu_sPOP$. This is easily justified by the fact that P–O(E) bond is significantly shorter than the P–O(L) bond.

(iii) Frequencies appearing in the IR-spectrum should be assigned to A modes

(iv) The modes which belong to A (Ra) and B (IR + Ra) species in $SrK_2P_4O_{12}$ appear as single bands in the IR-spectrum of $[NH_3(CH_2)_4NH_3]_2P_4O_{12}.9/2H_2O$, whereas the modes belonging to the E species should split into doublets

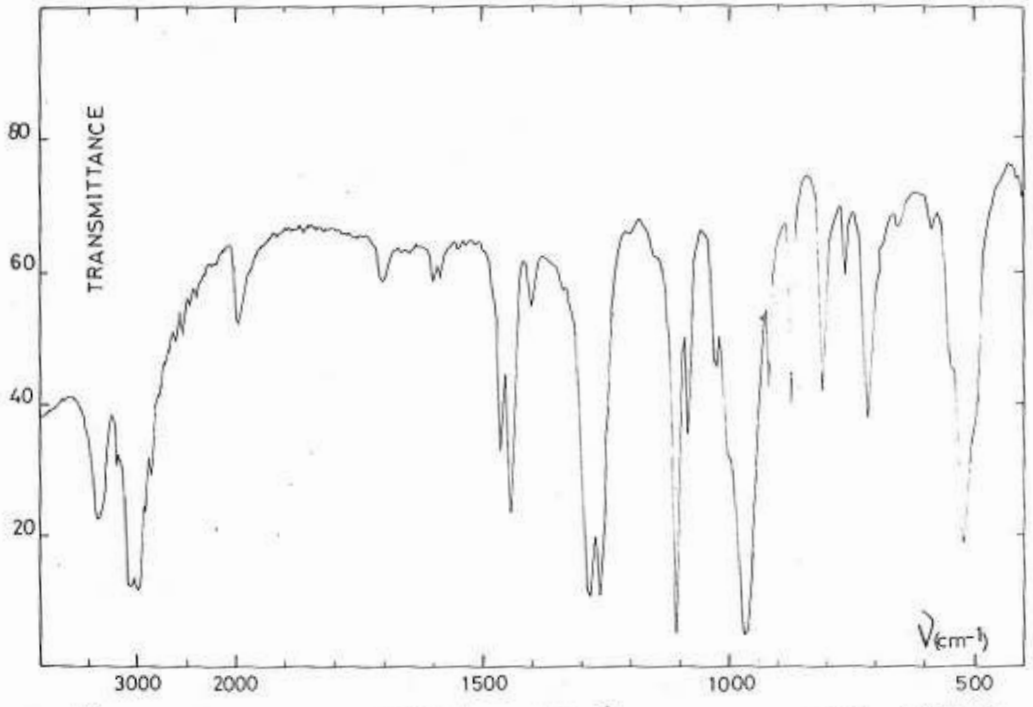

Figure 6: *IR spectrum of polycrystalline* $[NH_3(CH_2)_4NH_3]_2P_4O_{12}.9/2H_2O$

Moreover these rules should not be applied too strictly for evident reason: when the primitive cell contains several P_4O_{12} groups the increase in the number of bands may be not only due to a symmetry lowering, but to vibrational coupling between equivalent groups.

The assignments proposed for the P_4O_{12} stretching vibrations (table V) are consistent with these rules and can be pointed out in the following description:

— A doublet (1285-1260 cm^{-1}) with two additional weak bands at 1340 cm^{-1} and 1200 cm^{-1} are assigned to the asymmetric stretching vibration $\nu_{as}OPO^-$.

— A strong band (1110 cm^{-1}), a medium one (1083 cm^{-1}) and a shoulder (1150 cm^{-1}) correspond to the symmetric stretching vibration $\nu_{S}OPO^-$.

— The asymmetric stretching vibrations $\nu_{as}POP$ are characterized by a doublet (1030-1025 cm^{-1}) and a strong band at 965 cm^{-1} accompanied by a shoulder at 1000 cm^{-1}.

— A doublet (760-720 cm^{-1}) with a weak component and a medium one is observed with two bands at 805 cm^{-1} (medium) and 660 cm^{-1} (weak). These frequencies are attributed to the symmetric stretching vibration ν_sPOP.

All the assignments proposed here belong to the A species. On the basis of the observed and calculated frequencies [16] for $SrK_2P_4O_{12}$ with S_4 ring symmetry and taking into account the approximate character of these calculations, the agreement between these calculated frequencies and our own assignments is satisfactory for the stretching modes (cf.table V).

A tentative assignment for bands arising out of the P_4O_{12} stretching domain as proposed in table VI, is obtained by comparison with spectra of other organic and inorganic compounds, [20-25]. The domain of high frequencies in the spectrum is characterized by N(O)-H stretching and bending modes, combination bands and harmonics, while the low frequencies correspond to the bending and external modes.

The two supplementary-bands at 915 and 870 cm^{-1}, observed in the P_4O_{12} stretching domain, suggest a partial vibrational coupling between the equivalent P_4O_{12} rings present in the cell. Also these bands may be attributed to $\nu_{C\text{-}C}$ vibrations.

VI-CONCLUSION

$[NH_3(CH_2)_4NH_3]_2P_4O_{12}.9/2H_2O$ has been prepared at room temperature starting from aqueous solutions of $H_4P_4O_{12}$ and $NH_2(CH_2)_4NH_2$ and then crystallized by evaporation. The stoichiometry of the salt was confirmed by physico-chemical analysis and then the structure was elucidated by X-ray diffraction. It reveals that the putrescinium dications

$[NH_3(CH_2)_4NH_3]^{2+}$ have a strong preference to occupy crystallographic inversion centres or, if not, a general position but in a symmetric conformation with a non-crystallographic inversion centre. All N-H···O hydrogen bonds are between adjacent layers while the O-H···O bond operates within the anion layer. Water molecules assume three different roles: (i) linking two P_4O_{12} groups to form a cluster, (ii) connecting adjacent clusters in infinite ribbons along the b axis and (iii) allowing cohesion between ribbons of the layer. This is in good agreement with the DSC investigation: the total dehydration occurs in a wide temperature

Table V: *Vibrational frequencies and assignments in the P_4O_{12} stretching region. Factor group analysis and comparison with calculated frequencies for $SrK_2P_4O_{12}$ are also included.*

				$SrK_2P_4O_{12}$ [16]					$[NH_3(CH_2)_4NH_3]_2P_4O_{12}.9/2H_2O$				
	G.M.			G.S.			cm^{-1}		G.S.		cm^{-1}		
Mvt	D_{4h}	IR		S_4	IR	Ra	calc. IR	Ra		C_1	IR	obs.	
$\nu_{as}OPO^-$	A_{2u}	+	→	A	-	+	1260		→	A	+	1200	w
	B_{1u}	-	→	B	+	+	1290		→	A	+	1340	w
										A	+	1285	vs
	E_g	-	→	E	+	+	1270		⇄	A	+	1260	vs
$\nu_s OPO^-$	A_{1g}	-	→	A	-	+	1180		→	A	+	1150	sh
	B_{2g}	-	→	B	+	+	1080		→	A	+	1083	m
										A	+		
	E_u	+	→	E	+	+	1100		⇄	A	+	1110	vs
ν_{as} POP	A_{2g}	-	→	A	-	+	?		→	A	+	1000	sh
	B_{2g}	-	→	B	+	+	988		→	A	+	965	vs
										A	+	1030	m
	E_u	+	→	E	+	+	1000		⇄	A	+	1025	m
ν_s POP	A_{1g}	-	→	A	-	+	680		→	A	+	660	w
	B_{1g}	-	→	B	+	+	820		→	A	+	805	m
										A	+	715	m
	E_u	+	→	E	+	+	710		⇄	A	+	700	w

vs=very strong, s=strong, m=medium, w=weak, sh=shoulder

Table VI: *Tentative assignments of the observed IR frequencies outside the stretching domain of P_4O_{12} rings.*

$\bar{\nu}$ (cm^{-1})	assignments	$\bar{\nu}$ (cm^{-1})	assignments
3430 vs 3200 s 3080 vs 3010 vs 2950 s 2880 m	$\nu\ OH_2 + \nu\ NH_3^+ + \nu\ CH_2$	1150 w 915 m 870 m	ν C-C + ν C-N
2720 w 2620 w 2480 w 2550 vw	combined bands and harmonics	690 sh 675 w 585 m 545 s 520 vs 460 sh 405 m	deformation + external modes
1720 vw 1700 m 1665 vw 1645 vw 1625 vw 1600 m 1585 m 1550 w 1465 vs 1425 vs 1400 m	$\delta\ OH_2 + \delta\ NH_3^+ + \delta\ CH_2$		

vs= very strong,
s= strong,
m= medium,
w= weak,
vw= very weak,
sh= shoulder

range with three steps involving strongly different enthalpy values. This dehydration process can be related to the different types of water molecules as described above. IR investigation shows a fairly satisfactory agreement between the predicted, on the basis of a group theoretical analysis, and the observed P_4O_{12} stretching bands, especially in the 800-600 cm^{-1} characteristic region for C_1 symmetry.

REFERENCES

[1] M.T. Averbuch-Pouchot, A. Durif and J.C. Guitel, *Acta Crystallogr.*, 1988, **C44**, p.888.
[2] M.T. Averbuch-Pouchot, A. Durif and J.C. Guitel, *Acta Crystallogr.*, 1988, **C44**, p.1416.
[3] H. Thabet, M. Bdiri, A. Jouini and A. Durif, *J. Solid State Chem.*, 1992, **101**, p.211.
[4] M.T. Averbuch-Pouchot, A. Durif and J.C. Guitel, *Acta Crystallogr.*, 1989, **C45**, p.428.
[5] M. Bdiri and A. Jouini, *Acta Crystallogr.*, 1990, **C46**, p.1454.
[6] F. Takusagawa and T.F. Koetzle, *Acta Crystallogr.*, 1978, **B34**, p.1910.
[7] F. Takusagawa and T.F. Koetzle, *Acta Crystallogr.*, 1979, **B35**, p.867.

[8] S. Kamoun and A. Jouini, *J. Solid state Chem.*, 1990, **89**, p.67.
[9] E. Bartoszak and M. Jaskolski, *Acta Crystallogr.*, 1990, **C46**, p.2158.
[10] S. Furberg and J. Solbakk, *Acta Chem. Scand.*, 1972, **26**, p.2855.
[11] N.H. Woo, N.C. Seeman and A. Rich, *Biopolymers*, 1979, **18**, p.539.
[12] K. Chandrasekhar and V. Pattabhi, *Acta Crystallogr.*, 1980, **B36**, p.2486.
[13] M. Jaskoski, M. Alejska and M. Wiewiorowski, *J. Cryst. Spectrosc. Res.*, 1986, **16**, p.31.
[14] G. Charlot, "Chimie analytique quantique", **Vol. II**, 1974.
[15] Structure Determination Package RSX11M, 1979 Version, Enraf-Nonius, 1990.
[16] Kh.Kh. Muldagaliev, A.N. Lazarev and P. Mirgorodskii, *Inorg.Mat.* (Engl.Transl.), 1974, **10(4)**, p.563.
[17] V. Lutsko, I. Shashkova, E. Prodan and G. Peslyak, *Spectrochimica Acta*, 1986, **42A(8)**, p.851.
[18] P. Tarte, A. Rulmont, K. Sbai and M.H. Simono-Grange, *Spectrochimica Acta*, 1987, **43A(3)**, p.337.
[19] G. Fomakoye, R. Cahay and P. Tarte, *Spectrochemica Acta*, 1990, **46A**, p.1245.
[20] F. Scheinmann, "An introduction to spectroscopic Methods for the Determination of Organic Compounds, **Vol.I**, Pergamon, New York, 1970.
[21] N.B. Colthup, L.H. Daly and S.E. Wilberley, "Introduction to infrared and Raman spectroscopy", Academic Press (2nd edition), 1975.
[22] Z. Iqbal, H. Arend and P. Wachter, *J. Phys. C. Solid State Phys.*, 1981, **14**, p.1497.
[23] S. Skaarup and W. Berg, *J. Solid State Chem.*,1978, **26**, p.59.
[24] D. Philip and G. Aruldhas, *J. Solid State Chem.*, 1989, **83**, p.198.
[25] Y. Abid, M. Kamoun, A. Daoud and F. Romain, *J. Raman Spectrosc.*,1990, **21**, p.709.